Thin Solid Films 517 (2008) 990–993

Contents lists available at ScienceDirect

Thin Solid Films

journal homepage: www.elsevier.com/locate/tsf

A method of producing small grain Ru intermediate layers for perpendicular magnetic media

Hua Yuan *, Yueling Qin, David E. Laughlin

Materials Science and Engineering Department, Data Storage Systems Center, Carnegie Mellon University, 5000 Forbes Avenue, Pittsburgh, PA 15213, USA

ARTICLE INFO

Article history:
Received 28 May 2007
Received in revised form 9 June 2008
Accepted 24 July 2008
Available online 29 July 2008

Keywords:
Perpendicular magnetic media
Ru intermediate layer
Small grain size
Composite seedlayer

ABSTRACT

NiAl+SiO_2 thin films were used as a grain size reducing seedlayer for cobalt alloy granular perpendicular magnetic recording media. The effect of this NiAl+SiO_2 seedlayer on the microstructure and crystalline orientation of Ru intermediate layer has been investigated. By co-sputtering the composite NiAl+SiO_2 seedlayer, the smallest average grain diameter of NiAl was significantly reduced to about 2.5 nm. The grain size of the subsequent Ru intermediate layer was reduced to about 4 nm. X-ray diffraction results indicate an epitaxial orientation relationship of NiAl (110) // Ru (0002) between the two layers. Moreover, significant improvement of this epitaxial relationship was developed, which produced narrow *c*-axis distribution of the Ru intermediate layer with small grain size. The addition of the NiAl+SiO_2 seedlayer is a very promising approach to reduce the Ru intermediate layer grain size and eventually the magnetic layer grain size for perpendicular magnetic recording media without deterioration of other properties of thin films.

Published by Elsevier B.V.

1. Introduction

The microstructure of thin film magnetic recording media has been changing over the years to keep up with the ever increasing density of recording. It is controlled mainly by underlayers or intermediate layers which lie beneath the magnetic layer of the recording media and control the magnetic layer's crystallographic orientation and grain size [1].

B2 underlayers (NiAl, RuAl etc.) were introduced in the mid-1990s and because of the high binding energy of Ni and Al (or Ru and Al), the thin films of B2 materials usually have smaller grain size than the Cr underlayers [2–4].

Today, all media is perpendicular [5–7], using intermediate layers such as Ru and the media layer is a mixed layer of an oxide (e.g. SiO_2, TiO_2) and a Co based HCP (hexagonal-close-packed) magnetic alloy [8,9]. The Ru obtains a strong (0002) texture and enables the Co alloy to have its *c*-axis strongly oriented perpendicular to the film. The lattice mismatch between Ru and the Co alloy (in plane tensile strain) also helps to increase the effective anisotropy of the film.

The grain size of perpendicular magnetic media can be controlled by sputtering conditions and the amount of oxide in the thin magnetic film [10]. Also, it is effectively controlled by the grain morphology of the Ru intermediate layer which is usually deposited under high pressure condition [11]. The smaller the grain size in the intermediate layer, the smaller are the magnetic grains. Thus, obtaining small Ru grains in the intermediate layer is very important to ultimately reduce the magnetic grain size. Recently, various approaches have been made to further reduce this size while maintaining the competitive recording properties of the media by engineering the intermediate layers under the hard recording layer. It was reported that the magnetic grain size was reduced to 5.8 nm with a synthetic nucleation layer (SN) between Ru1 and Ru2 layers [12], or 5.9 nm with an ultrathin nucleation site layer (NSL) under a stacked Ru layer [13], or 6.4 nm with a RuCr: oxide intermediate layer [14]. Also, oxide additions to the Ru intermediate layers are very likely to effectively reduce the grain size with better grain isolation at thinner thickness [11,15]. In this paper we report on our use of NiAl+oxide seedlayers to reduce the grain size of the magnetic recording media.

2. Experimental procedure

In order to produce magnetic thin films with strong perpendicular orientation of the easy axis and very small grain size, we introduce the use a seedlayer composed of a high melting point phase (such as NiAl, B2 structure) mixed with an amorphous SiO_2 phase to reduce the grain size of the NiAl films. This seedlayer acts as a template for the intermediate Ru layer to produce small Ru grains which are in contact with the magnetic grains. Fig. 1 is a schematic illustration of our proposed small grain perpendicular recording media. It is composed of an amorphous adhesion layer (Ta), a seedlayer I (Ru I) and seedlayer II (NiAl+SiO_2), an intermediate layer (Ru II) (non-magnetic), followed by the magnetic layer and an overcoat layer.

Table 1 is the list of the thin film samples: (1) Ta (4 nm)/NiAl+SiO_2 (15 nm)/Ru II (t=0, 3, 5, 10, 15 nm); (2) Ta (4 nm)/Ru I (15 nm)/Ru II (t=5 nm); and (3) Ta (4 nm)/Ru I (15 nm)/NiAl+SiO_2 (15 nm)/Ru II (t=0, 5 nm). They were prepared by radio frequency diode sputtering on naturally oxidized silicon substrates with 6.0×10^{-5} Pa base

* Corresponding author. Tel.: +1 412 268 2458; fax: +1 412 268 3113.
E-mail address: huay@andrew.cmu.edu (H. Yuan).

0040-6090/$ – see front matter. Published by Elsevier B.V.
doi:10.1016/j.tsf.2008.07.032

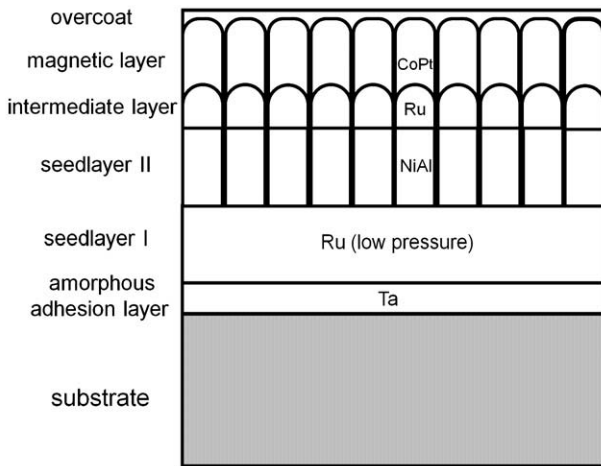

Fig. 1. Schematic illustration of small grain granular perpendicular magnetic recording media.

pressure using a Leybold-Heraeus Z-400 sputtering system. The Ta and Ru layers were directly sputtered and deposited on the substrate from elemental targets. The seedlayer I (Ru I) layer was sputtered at very low Ar sputtering pressure to produce strong (0002) texture and a smooth surface, while the intermediate layer (Ru II) was sputtered at a much higher Ar sputtering pressure to produce better isolation of the magnetic grains. The relative amount of NiAl and SiO_2 was controlled by changing the surface area of the chips of SiO_2, which were mounted on a NiAl alloy target. The nominal composition of films NiAl+SiO_2 was estimated after obtaining the deposition rate of the two materials. For all the samples in this study, the SiO_2 content in the NiAl+oxide layer was fixed at 18 vol.% (volume fraction) and this seedlayer was sputter deposited at 1.3 Pa Ar pressure. The crystallographic orientation of the films was measured using X'Pert X-ray diffractometer with Cu Kα radiation. The thin film microstructure was investigated using a JOEL 2000 and a FEI Tecnai F20 transmission electron microscopes (TEM).

3. Results and discussion

In this work, the feasibility of NiAl+SiO_2 film as a grain size reduction seedlayer for the epitaxial growth of Ru intermediate layer was studied in terms of crystallographic structure and microstructure. The (110) NiAl (a=2.887 Å) surface exhibits the lowest surface energy of about 1.80 J/m^2 [16–18]. This low energy surface suggests a favorable development of (110) orientation upon sputtering. The lattice mismatch between the HCP Ru (a=2.71 Å) (0002) plane and NiAl (110) plane is about 7.33%. A schematic plot of their crystalline orientation relationship is shown in Fig. 2.

Fig. 3(a) shows the XRD θ–2θ patterns of films: (1) Ta (4 nm)/NiAl+SiO_2 (15 nm)/Ru II (t=0, 3, 5, 10, 15 nm) where Ta was deposited as the amorphous adhesion layer. NiAl (110) was observed to have a very

Table 1
List of the samples sputter deposited on naturally oxidized silicon wafer

Samples	Layer 1	Layer 2	Layer 3	Layer 4
1-1	Ta (4 nm)	N/A	NiAl+SiO_2 (15 nm)	N/A
1-2	Ta (4 nm)	N/A	NiAl+SiO_2 (15 nm)	Ru II (3 nm)
1-3	Ta (4 nm)	N/A	NiAl+SiO_2 (15 nm)	Ru II (5 nm)
1-4	Ta (4 nm)	N/A	NiAl+SiO_2 (15 nm)	Ru II (10 nm)
1-5	Ta (4 nm)	N/A	NiAl+SiO_2 (15 nm)	Ru II (15 nm)
2	Ta (4 nm)	Ru I (15 nm)	N/A	Ru II (5 nm)
3-1	Ta (4 nm)	Ru I (15 nm)	NiAl+SiO_2 (15 nm)	N/A
3-2	Ta (4 nm)	Ru I (15 nm)	NiAl+SiO_2 (15 nm)	Ru II (5 nm)

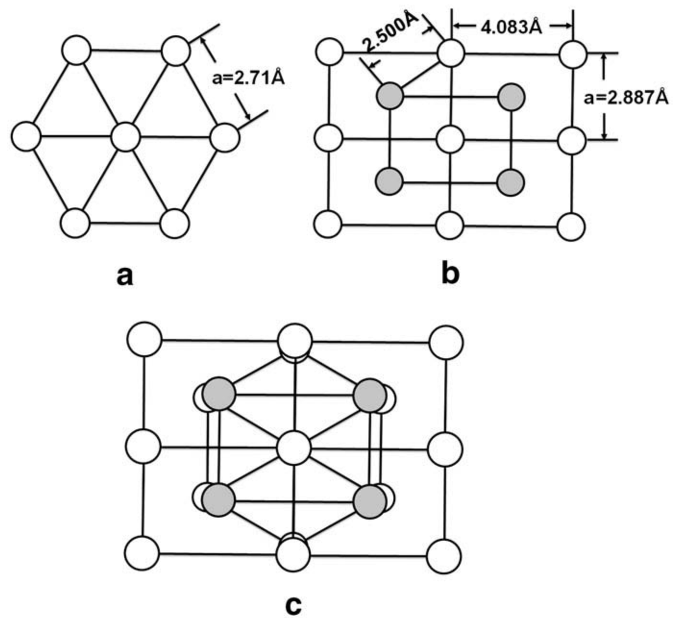

Fig. 2. Schematic illustration of (a) the (0002) plane of HCP Ru (a=2.71 Å); (b) (110) plane of B2 NiAl (a=2.887 Å); and (c) the crystalline orientation relationships between (0002) plane of Ru and (110) plane of NiAl.

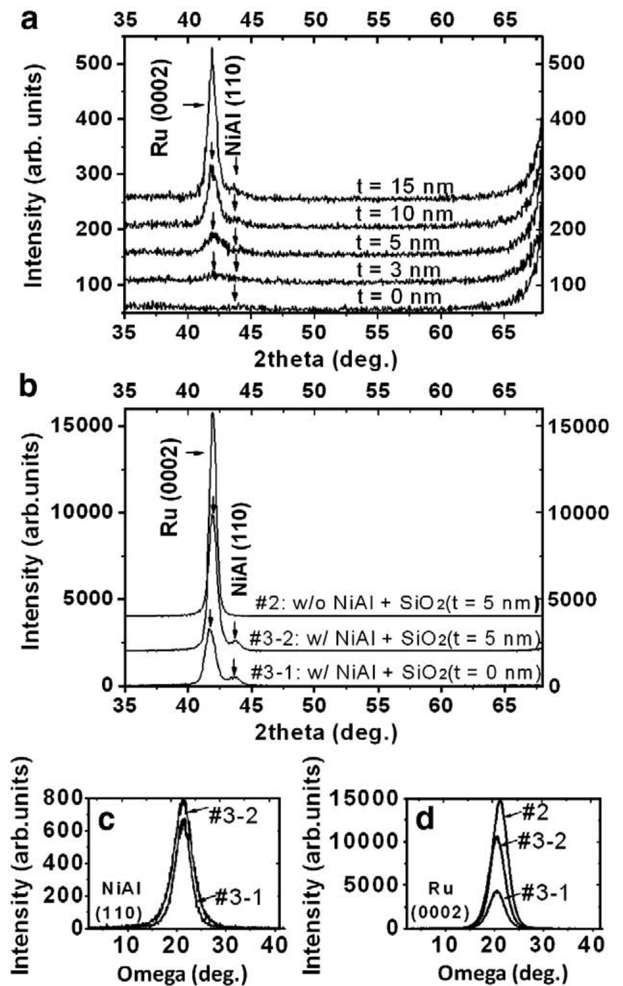

Fig. 3. (a) XRD patterns of thin films: #1 substrate/Ta (4 nm)/NiAl+SiO_2 (15 nm)/Ru II (t=0, 3, 5, 10, 15 nm) respectively; (b) XRD patterns of thin films: #2 substrate/Ta (4 nm)/ Ru I (15 nm)/Ru II (t=5 nm) and #3 substrate/Ta (4 nm)/Ru I (15 nm)/NiAl+SiO_2 (15 nm)/ Ru II (t=0, 5 nm) respectively; (c) and (d) are the ω-rocking curves of NiAl (110) and Ru (0002) diffraction peaks respectively for samples corresponding to (b).

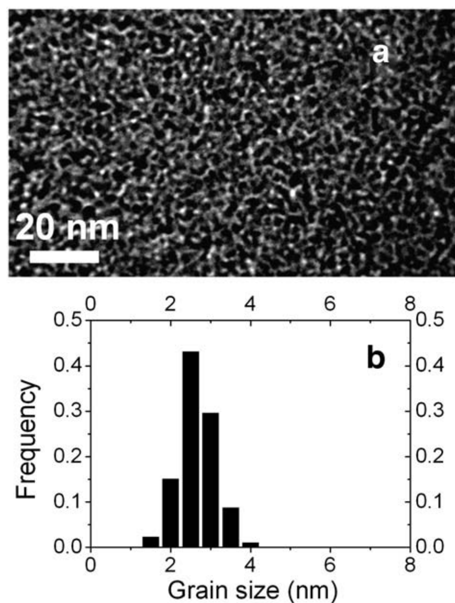

Fig. 4. TEM plan-view image of (a) NiAl + SiO_2 in seedlayer II (the white regions are the amorphous phase of SiO_2) and (b) the grain size analysis based on image (a).

weak intensity when deposited on the Ta layer, although Ru (0002) developed stronger intensity with increasing thickness from 0 nm to 15 nm. This indicates that NiAl grains orientate more randomly around the <110> axis, although most of (110) planes are parallel to the film plane. Ru preferentially favors the (0002) texture for better lattice match.

Fig. 3(b) shows the XRD patterns of (2) Ta (4 nm)/Ru I (15 nm)/Ru II (t=5 nm); and (3) Ta (4 nm)/Ru I (15 nm)/NiAl + SiO_2 (15 nm)/Ru II (t=0, 5 nm). In these samples, another Ru I seedlayer was added to enhance the NiAl (110) texture in light of the orientation relationship in Fig. 2. It can be seen that without any seedlayer NiAl + SiO_2, the film is the same as the dual layer Ru intermediate layers for current media [19]. The full width at half maximum (FWHM) value of the Ru (0002) rocking curve in this sample is 3.70°, which shows a very narrow c-axis distribution. For the sample: Ta (4 nm)/Ru I (15 nm)/NiAl + SiO_2 (15 nm), the Ru (0002) peak also has a 3.70° dispersion, while the NiAl (110) peak has 3.70° dispersion (see Fig. 3(c) and (d)). It is not surprising that the NiAl (110) orientation spread is small, since the peak sits on the tail of Ru (0002) from Ru I. Usually, they can hardly be de-convoluted from each other. However, judging from the significant intensity increment compared with the previous sets of samples in Fig. 3(a), the texture of the NiAl (110) is greatly improved by the Ru I layer addition and its dispersion is significantly narrower by an order of magnitude. A 5 nm thick Ru II intermediate layer was subsequently deposited on top of this sample. The spectra of two similar peaks have been observed (see Fig. 3(c) and (d)). The Ru (0002) peak at 2θ = 41.9° has a FWHM of 3.84° and NiAl (110) peak at 2θ = 43.6° has a FWHM of 4.41°. Obviously, the contribution of Ru peak intensity is from two separate layers. Also, the Ru II dispersion must be slightly larger than Ru I, although the degradation effect is very small. The difference of NiAl (110) FWHM reading can be explained by the Ru tail effect. However, once the thickness of the NiAl + SiO_2 was reduced to 7 nm, the FWHM of Ru (0002) and NiAl (110) rocking curves increased to 8.73° and 9.23°, respectively. All these results demonstrate a very good epitaxial relationship developed between adjacent layers and a narrow orientation distribution of these thin films, although an optimum thickness needs to be selected to balance the tradeoff between good perpendicular orientation and thinner overall seedlayer and intermediate layer thickness.

Fig. 4(a) is the plan-view TEM image of seedlayer II NiAl + SiO_2, showing the microstructural characteristics of this layer. It can be observed that the NiAl grains are physically separated by the SiO_2 phase in the film plane. SiO_2 forms fairly uniform boundaries with about 0.5–1.0 nm width. Based on this image, the grain size distribution analysis was performed as shown in Fig. 4(b). The average grain size of NiAl is ~2.5 nm and the standard deviation is ~0.2 nm. The grain size distribution is fitted with a log normal distribution curve, which suggests that the grain growth in this composite film is controlled by the finite surface drift and diffusion of atoms or species in the presence of two phase materials. It has been reported previously that NiAl thin films without oxide addition have larger average grain size of ~15 nm [20]. Our result shows that composite NiAl + SiO_2 layer yields very small grains. However, the grain isolation is not perfect in this seedlayer and some of the NiAl grains are interconnected with each other.

Cross-sectional TEM images of the Ru II intermediate layer are shown in Fig. 5. Fig. 5(a) shows the overall seedlayer and intermediate layer microstructure at low magnification. It is very clear to observe several columnar Ru grains in the intermediate layer with white grain boundaries on the top part of the left figure. The center-to-center Ru inter-grain distance is only around 4 nm. The feature size of Ru grains is about the same as that of NiAl grains in Fig. 4(a), since this value matches the 2.5 nm NiAl grains in the layer underlying. It is believed that the 1.5 nm difference in the feature size is probably due to the presence of about 18 vol.% SiO_2 phase as the NiAl grain boundaries. During the nucleation and growth process of the thin film, the metal atoms tend to grow on the other metal atoms with proper lattice matching to form epitaxial columnar grains because of lower surface energy considerations. The more random arrangement of Ru atoms is prone to form on low energy oxide phase around the NiAl grain

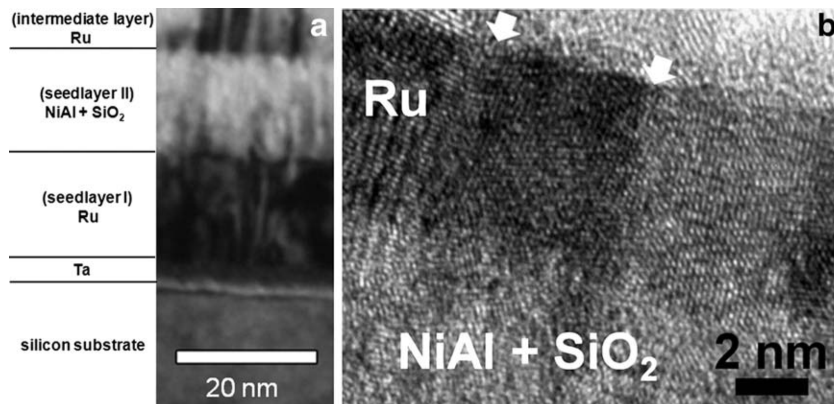

Fig. 5. (a) TEM cross-sectional image of sample: substrate/Ta (4 nm)/Ru I (15 nm)/NiAl + SiO_2 (15 nm)/Ru II (t=5 nm); (b) high resolution TEM cross-sectional image of Ru intermediate layer of sample: substrate/NiAl + SiO_2 (15 nm)/Ru II (t=5 nm) respectively.

boundaries to minimize the surface energy as well. Consequently, there might be a one to one grain growth between the NiAl + SiO_2 layer and Ru II intermediate layer in light of energy minimization between interfacial epitaxial growth of texture films.

Fig. 5(b) shows the high resolution TEM image of the interface between NiAl + SiO_2 and Ru II intermediate layer. The noticeable feature of crystal lattices with equal spacing can be observed where the well-defined Ru grains are present on the top part of this figure. The random regions between the grains are the grain boundaries indicated by the white arrows. The NiAl grains cannot be distinguished very clearly in either the low magnification or the high resolution TEM images. There are several reasons: (1) at low magnification, the scattering factor and mass for NiAl and SiO_2 are very close, therefore, the dark and light feature is not evident for this particular layer; (2) at high magnification, due to the nature of very small size of NiAl grains, along the direction perpendicular to the image, oxide boundary and grain are very likely to overlap with each other. Thus the ultimate image is the convolution of two parts' contributions. A well-defined granular morphology can barely be seen from cross-sectional view. However, the plan-view image of this layer in Fig. 4(a) is sufficient to demonstrate the real microstructure.

4. Conclusions

This study has introduced a method of producing small Ru grains in the intermediate layer for future perpendicular magnetic recording media. A seedlayer consisting of NiAl + SiO_2 has been developed with a very small grain size of about 2.5 nm. Subsequently, the grain size of Ru intermediate layer was reduced to about 4 nm. XRD patterns show that Ru grains grow with a crystalline orientation relationship on the NiAl grains, which indicates the texture matching of (0002) Ru and (110) NiAl. Also, the Ru I seedlayer I deposited at low pressure was found to significantly enhance the (110) NiAl + SiO_2 epitaxial thin films. As a result, strong (0002) texture of Ru with isolated columnar-shaped grains in the intermediate layer fabricated at higher Ar pressure can be produced with smaller grain size. This result suggests that the magnetic layer which is subsequently sputtered on the Ru intermediate layer will have small grain size and strong texture which are necessary to produce perpendicular recording media with low noise and high recording density.

Acknowledgements

This work was in part supported by the Seagate Research, Pittsburgh, PA and the Data Storage Systems Center of CMU. The authors would like to thank Dr. Bin Lu and Dr. Yingguo Peng of Seagate Research and Prof. Jimmy Zhu of CMU for helpful discussions.

References

[1] B. Lu, D.E. Laughlin, Microstructure of Longitudinal Media, The Physics of Ultrahigh-Density Magnetic Recording, Springer Series in Surface Sciences, vol. 41, Springer-Verlag, Berlin, 2001.
[2] L.-L. Lee, D.N. Lambeth, D.E. Laughlin, U.S. Patent No. 5693426, 2 Dec. 1997.
[3] Q. Chen, Z. Wu, S.D. Harkness, IV, R.Y. Ranjan, U.S. Patent No. 6908689, 21 June 2005.
[4] Y. Ikeda, Y. Sonobe, G. Zeltzer, B.K. Yen, K. Takano, H. Do, E.E. Fullerton, P. Rice, IEEE Trans. Magn. 37 (2001) 1583.
[5] K. Hayashi, M. Hayakawa, H. Ohmori, A. Okabe, K. Aso, J. Appl. Phys. 67 (1990) 5175.
[6] T. Hikosaka, T. Komai, Y. Tanaka, IEEE Trans. Magn. 30 (1994) 4026.
[7] T. Oikawa, M. Nakamura, H. Uwazumi, T. Shimatsu, H. Muraoka, Y. Nakamura, IEEE Trans. Magn. 38 (2002) 1976.
[8] H. Uwazumi, K. Enomoto, Y. Sakai, S. Takenoiri, T. Oikawa, S. Watanabe, IEEE Trans. Magn. 39 (2003) 1914.
[9] E. Girt, S. Wu, B. Lu, G. Ju, T. Nolan, S. Harkness, B. Valcu, A. Dobin, J.D. Risner, M. Munteanu, R. Thangaraj, C.-H. Chang, T. Tran, X. -Wu, O. Mryasov, D. Weller, S. Hwang, J. Appl. Phys. 99 (2006) 08E715.
[10] S.H. Park, S.O. Kim, T.D. Lee, H.S. Oh, Y.S. Kim, N.Y. Park, D.H. Hong, J. Appl. Phys. 99 (2006) 08E701.
[11] I. Takekuma, R. Araki, M. Igarashi, H. Nemoto, I. Tamai, Y. Hirayama, Y. Hosoe, J. Appl. Phys. 99 (2006) 08E713.
[12] S.N. Piramanayagam, J. Appl. Phys. 102 (2007) 011301.
[13] R. Mukai, T. Uzumaki, 10th Joint MMM/Intermag Conference, Baltimore, U.S.A., January 7–11, 2007, 2007, p. 279, abstract No. EB-05.
[14] S.N. Piramanayagam, J.Z. Shi, H.B. Zhao, C.K. Pock, C.S. Mah, C.Y. Ong, J.M. Zhao, J. Zhang, Y.S. Kay, L. Lu, IEEE Trans. Magn. 43 (2007) 633.
[15] U. Kwon, R. Sinclair, E.M.T. Velu, S. Malhotra, G. Bertero, IEEE Trans. Magn. 41 (2005) 3193.
[16] R. Yu, P.Y. Hou, Appl. Phys. Lett. 91 (2007) 011907.
[17] A.Y. Lozovoi, A. Alavi, M.W. Finnis, Comput. Phys. Commun. 137 (2001) 174.
[18] A.T. Hanbicki, A.P. Baddorf, E.W. Plummer, B. Hammer, M. Scheffler, Surf. Sci. 331–333 (1995) 811.
[19] R. Mukai, T. Uzumaki, A. Tanaka, J. Appl. Phys. 97 (2005) 10N119.
[20] L.-L. Lee, D.E. Laughlin, D.N. Lambeth, IEEE Trans. Magn. 30 (1994) 3951.